Heliyon 9 (2023) e19595

Contents lists available at ScienceDirect

Heliyon

journal homepage: www.cell.com/heliyon

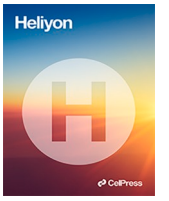

Incorporation of thermally induced shaped and phases of manganese oxide nanoparticles into zein/PVA fiber blends

Nompumelelo S.M. Kubheka, Makwena J. Moloto *

Institute for Nanotechnology and Water Sustainability, College of Science, Engineering and Technology, University of South Africa, Florida Park Campus, 1709, South Africa

ARTICLE INFO

Keywords:
Zein
Poly(vinyl alcohol) (PVA)
Fiber blends
Manganese oxide
Nanoparticles

ABSTRACT

Incorporation of nanomaterials into polymers and their blend provide additional advantages to their use and structural support. Metals such as Ag, Cu, Ti, and Fe are often reported in their metallic or their oxide forms for applications in microbiological, water treatment, and biomedical fields. The integration of metal oxide nanoparticles into polymer fiber blends overcomes the mechanical instability and compatibility challenges of nanomaterials. Manganese-based oxides provide good stability and optical properties in their nanoscale useful in polymeric composite or fiber materials enhancement. MnO_2 and Mn_2O_3 nanoparticles were synthesized at different calcination temperatures using the co-precipitation method and characterized a microscopic technique TEM, and TGA. TEM images and the XRD patterns confirmed that the manganese oxide nanoparticle were spheres and rod-shaped with corresponding cryptomelane and orthorhombic crystalline phases. Mn_2O_3 nanoparticles were successfully integrated into zein/PVA (80/20) fiber blends. SEM images confirmed that the inclusion of the nanoparticles into zein/PVA solutions increased the conductivity of the solutions which led to an improved morphology and increased surface area to volume ratio. XRD patterns and TGA showed that the incorporated nanoparticles were below the detection limit, therefore there was no significant change observed. Therefore, all characterization techniques illustrated that the effect of concentration significantly enhanced the morphology of the fiber blends.

1. Introduction

In recent years, extensive research has focused on nanocomposites made of inorganic nanoparticles in polymer matrices. Metal oxides are extremely attractive candidates among the nanomaterials that can be synthesized at the nanometric scale. Due to modifications in their structure and interactions, these oxides exhibit intriguing electrical and magnetic characteristics. Manganese oxide is regarded as the most complicated metal oxide. There are different types of manganese oxides such as manganite (MnO), hausmannite (Mn_3O_4), bixbyite (Mn_2O_3), and pyrolusite (MnO_2), and the metastable Mn_5O_8 is the most stable oxide produced. The oxidation process is usually governed by the diffusion of oxygen, During the oxidation process, these oxides may coexist or gradually transform one into the other [1]. The synthesis of polymorphs manganese oxide (Mn_2O_3) nanoparticles has been demonstrated to be affordable, environmentally friendly and a catalyst that is appropriate for the oxidation of persistent organic pollutants and the degradation of nitrogen oxide [2,3]. There are different methods utilized to synthesize manganese oxide nanoparticles including the thermal

* Corresponding author.
E-mail address: molotmj@unisa.ac.za (M.J. Moloto).

https://doi.org/10.1016/j.heliyon.2023.e19595
Received 26 June 2023; Received in revised form 23 August 2023; Accepted 28 August 2023
Available online 29 August 2023

decomposition, permanganates reduction, adsorption–oxidation, exfoliation strategy, and hydrothermal or solvothermal method [2].

The incorporation of nanoparticles into polymeric fibers is an effective process to enhance the physicochemical properties of polymers. In addition, polymeric nanofibers embedded with composite nanoparticles retain their structural properties and the problem associated with nanoparticle dispersion on the surface of nanofibers does not exist [4]. The characteristics of polymer fibers such as their morphological structure, size distribution, concentration and interactions are influenced by the type of nanoparticles embedded [5]. Zein is a natural polymer with intriguing properties such as durability, pliability, compressibility, and it is hydrophobic because of the presence of apolar amino acids [6]. However, zein exhibits inadequate mechanical stability therefore, it is essential to enhance the mechanical properties of zein by blending it with a synthetic polymer such as poly (vinyl alcohol). PVA is made up of carbon-carbon bonds and hydroxyl groups, resulting in it being a highly stable hydrophilic polymer [7]. It is a suitable additive for zein because of its strong optical and physiochemical properties [8]. Electrospinning is a versatile technique utilized by many researchers in numerous sectors. Electrospun nanofibers have highly distinct features compared to any other known form of the material due to their flexibility in surface functionalities, superiority in mechanical performance and high surface to ratio area. The electrospinning technique has become very popular over the past few decades [8,9]. Electrospinning process parameters include the TCD, electric field, and velocity of solution flow; all these process parameters have an impact on the fabrication of the electrospun nanofibers [10,11]. The fabrication of polymer fiber blends is a good alternative and inexpensive process, it ensures that future energy and environmental sustainability are guaranteed. However, none has been reported on the synthesis of permanganate reduction method and incorporation of manganese oxide (Mn_2O_3) nanoparticles into zein/PVA fiber blends. Therefore, this paper describes the synthesis of the manganese oxide nanoparticles via the co-precipitation method varying different calcination temperatures in the view of morphology, size, and diameters. Furthermore, the effect of adding different concentrations of Mn_2O_3 into electrospun zein/PVA was investigated.

2. Experimental

2.1. Materials

All chemicals were purchased from Sigma-Aldrich (Merck) and were used as received. These are Zein (Mw 3.5×10^4), Polyvinyl alcohol (PVA) (Mw 89,000–98,000, 99%, hydrolyzed), and ethanol, potassium permanganate ($KMnO_4$) and ammonium solution ((NH_3, 28.0–32.0%).

2.2. Methodology

2.2.1. Synthesis of manganese oxide nanoparticles by co-precipitation method

Potassium permanganate (0.126 g) was dispersed in 95 ml of dilute ammonium solution in a 100 ml beaker. The solution was stirred with a magnetic stirrer bar for 15 min to dissolve potassium permanganate. The stirring was stopped, and the solution was transferred into centrifuge tubes and stored at room temperature for 24 h in the dark. The produced precipitate was washed using distilled H_2O for five intervals and separated by centrifugation at 6000 rpm for 5 min. The precipitate was crushed into fine particles and calcined at 600 and 800 °C using the furnace.

2.2.2. Electrospinning

The weight ratio of zein/PVA was fixed at 80:20 in 70% ethanol solution. Various concentrations of bixbyite nanoparticles in the range of (4.25–5.25%) were added to the zein/PVA solution. The combined solution was stirred for 24 h on a magnetic stirrer until the solution was homogeneous. Electrospinning was performed at room temperature with a voltage of 25 kV and a tip-to-collector distance (TCD) of 10 cm. A syringe pump was used to feed the polymer solution into the needle tip at a rate of 0.050mm/min.

2.3. Characterization of nanoparticles and electrospun nanocomposite fibers

A JEOL JEM-2100 transmission electron microscope operating at 200 kV was used to obtain the size and shape of the synthesized iron oxide and manganese oxide nanoparticles. The crystallinity and size of nanoparticles and nanocomposite fibers were confirmed using a Bruker D2 diffractometer (40 kV and 50 mA) and secondary graphite monochromatic (Co K-alpha radiation $l = 1.7902$ Å). Surface morphologies of zein/PVA nanofiber blends were studied using a FE-SEM microscope at 1.00 keV electron potential. The optical properties of nanoparticles and nanocomposite fibers were studied using a Thermo Scientific Evolution 220 UV visible spectrophotometer, which collects spectra in the wavelength range of 1100–190 nm using a spectral bandwidth of 1 nm (variable slit) to determine the absorption spectra of the prepared nanoparticles before and after incorporation into the polymer fibers. The Thermo Scientific Nicolet iS50-FTIR spectrometer (ATR-diamond detector) was used to study the chemical structure, interaction and composition of zein/PVA/Mn_2O_3 nanocomposites. Additionally, the thermal stability of the fabricated polymer fiber nanocomposite was analyzed using a PerkinElmer STA 600 Simultaneous Thermal Analyzer (Waltham, USA). An inert nitrogen atmosphere, 20 ml/min flow rate (3.2 bar), and at a heating rate of 10 °C/min starting from 30 to 900 °C was used for this analysis. used.

3. Results and discussion

3.1. Effect of temperature on manganese oxide nanoparticles

3.1.1. Optical properties

Monodisperse manganese oxide nanoparticles have been previously reported before using more complex methods which require high temperatures with autoclave, complicated multi-step synthetic procedure, and capping agents [1–3]. In this study, no capping agents were utilized to form monodisperse nanoparticles which contain potassium ions within the tunnels (K-OMS-2/Mn_xO_y) octahedral molecular sieve (OMS). The manganese oxide nanoparticles were prepared in a single-step precipitation method at room temperature respectively at pH 12 and were calcined at 600 and 800 °C. The optical properties in Fig. 1(A) and B illustrate the difference between the absorption spectra of the nanoparticles prepared at different temperatures and their band edge. The energy band edges estimated using the Tauc plot $((\alpha h\nu)^2$ Vs $h\nu)$ are observed at 2.41 eV (Fig. 1(C) and D) and 2.43 eV for MnO_2 and Mn_2O_3 calcined at 600 and 800 °C, respectively. The slight increase in the band gap energy of the manganese nanoparticles with increase in calcination temperature may be attributed to the potential particle size growth as per previous report [12]. The PL results displayed a blue-shifted peak of 421 nm for MnO_2 nanoparticles (calcined at 600 °C) as compared to the Mn_2O_3 (calcined at 800 °C) nanoparticles with a peak value of 454 nm. At 800 °C, a decrease in the maximum emission intensity was observed and could be attributed to the morphological change of the particles forming small non-spherical crystals. Previous reports shows that manganese oxide nanoparticles are expected to display optical features within the 300–600 nm wavelength range, which correlates with the PL and UV Visible results obtained in this study [13,14].

3.1.2. Morphological analysis

The manganese oxides, found in various oxidation states have been previously investigated for their electronic, magnetic properties and applications for the treatment of water [1–3]. Manganese oxide nanoparticles were prepared in a single-step precipitation method at room temperature without the addition of any protective agent, respectively at pH 12, and were calcined at 600 and 800 °C. In general, an increase in the temperature of calcination provides a high crystallinity hence manganese oxide nanoparticles were

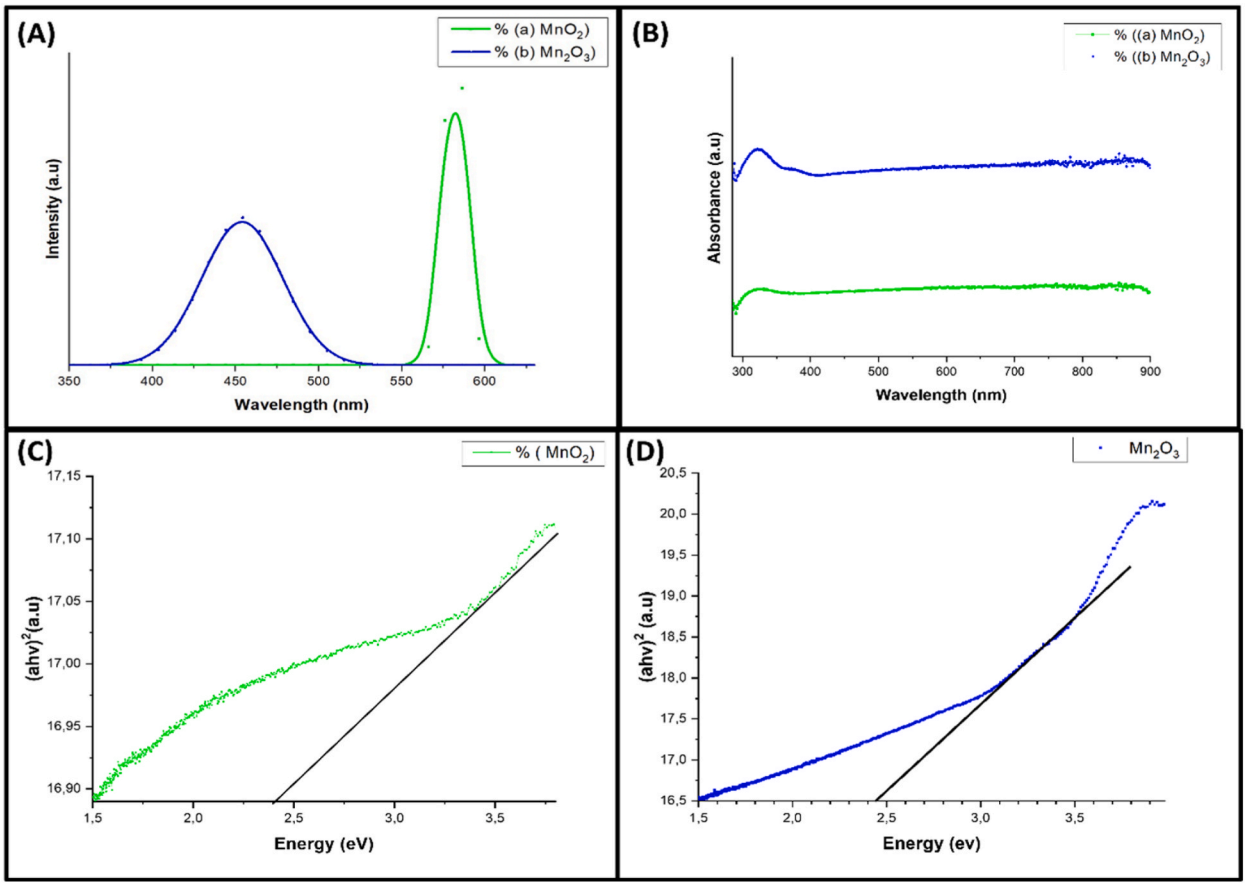

Fig. 1. Absorption (A), Emission (B) spectra, and Tauc plot (C–D) of manganese oxide nanoparticles calcined at high temperatures (a) 600 °C and (b) 800 °C.

synthesized at higher temperatures. Although, according to literature low temperature and pH fasten the transformation of Mn oxidation state between various polymorphs [15]. The TEM image and particle size distribution (Fig. 2(a), (b)) for particles prepared at 600 °C revealed uniform monodispersed spherical-shaped nanoparticles with a particle size distribution of 100–300 nm. The particles changed to a mixture of spheres and rods at the temperature was increased to 800 °C (Fig. 2(c)–(e)). This displayed polydispersity with particle size distribution of spheres and rods in the range of 20–80 nm and 50–300 nm, respectively. According to other findings [14, 16,17], there was a decrease in nanoparticle diameters with changing shape which is to favourable nucleation. Therefore, the chosen calcination temperatures of 600 and 800 °*C* formed highly crystalline manganese oxide nanoparticles without noticeable impurities of different manganese oxide phases.

The investigation of crystal structure of the monodisperse K-OMS-2/Mn_2O_3 octahedral molecular sieve (OMS) nanoparticles was analyzed using XRD spectra. The MnO_2 nanoparticles calcined at 600 °C displayed a prominent peak at 36° and not any other clear peak was displayed therefore it indicates the nanospheres are amorphous [18]. At an increased calcination temperature of 800 °C more dominant sharp peaks were displayed which illustrates that there was a change in crystalline size and the crystalline pattern. The peak observed in Fig. 3(a) corresponds to the cryptomelane phase with JCPDS No. 29–1020. Additionally, the were other peaks that corresponded to the orthorhombic phase of Mn_2O_3 (JCPDS No. 04-007-088) obtained after calcination at 800 °C (Fig. 3(b)). The XRD patterns not shown gave no features of the manganese nanoparticles. This could be attributed to the poor crystallinity of the polymer matrix they were loaded in. The hybrid electrospun manganese oxide/PVP nanofibers that were calcined at different temperatures (400 °C and 700 °C) to remove the polymer matrix, yielding inorganic MnO_x nanofibers with varied Mn_3O_4 to Mn_2O_3 compositions were studied in the article [16]. XRD results of the calcined MnO_x nanofibers corresponded to Mn_3O_4 (JCPDS 024–0734), Mn_2O_3 (JCPDS 073–1826), or a combination of the two. Nanofibers calcined at 400 °C adopted the tetragonal Mn_3O_4 phase. It was noted that an increase in the calcination temperature to 700 °C, Mn_3O_4 changed into more oxidized Mn_2O_3, yielding mixed-phase nanofibers (MnO_x nanofibers). This study confirmed calcined nanoparticles plays a significant role on electrospun nanofiber morphologies in particular affecting the diameter size as a result of concentration and crystalline phase. Therefore, concentration loading of nanoparticles into the polymer solution influences the signal detection limit of the XRD instrument.

3.2. *Manganese oxide nanoparticles embedded into the polymer blended fibers*

3.2.1. *Effect of Mn_2O_3 nanoparticles loadings embedded onto zein/PVA fiber blends*

The incorporation of manganese oxides into polymer fibers is of great interest in environmental remediation because of their low cost, less toxicity, and wide availability. Addition of nanoparticles enhances viscosity which has proven to have an effect on polymeric nanofiber diameters [17]. Fig. 4(a)–(d) of SEM images show the different concentrations of Mn_2O_3 nanoparticles embedded onto zein/PVA fiber blends under the optimized conditions (voltage, 25 kV, and TCD 10 cm). Fig. 4(a) revealed that the addition of Mn_2O_3 nanoparticles reduced the average size fiber diameter resulting in narrow nanocomposite fiber blends with an mean diameter of 793 ± 1.31 nm, the morphology appeared to be smooth with nanoparticles embedded onto zein/PVA polymer blend. Fig. 4(b) showed an increase in average fiber diameter of 1136 ± 1.32 nm upon increasing the nanoparticles loadings to 4.75 wt%. The morphology of the

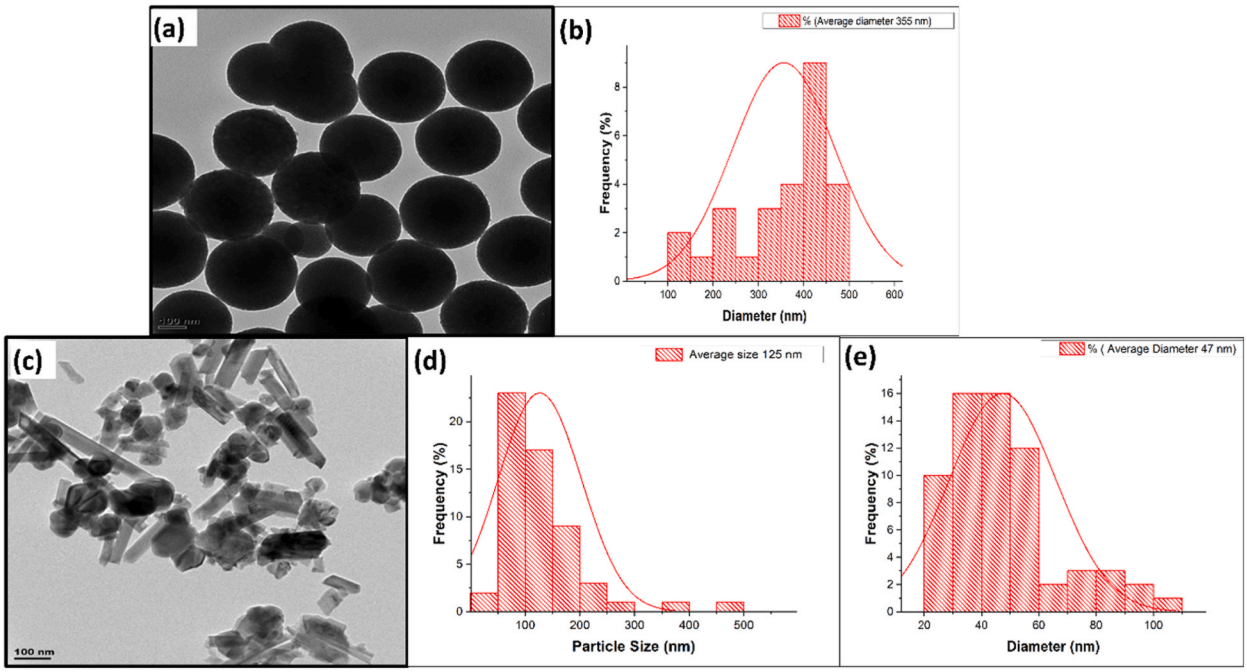

Fig. 2. TEM images and size distribution of manganese oxide nanoparticles calcined at high temperatures 600 °C (a, b) and 800 °C (c–e).

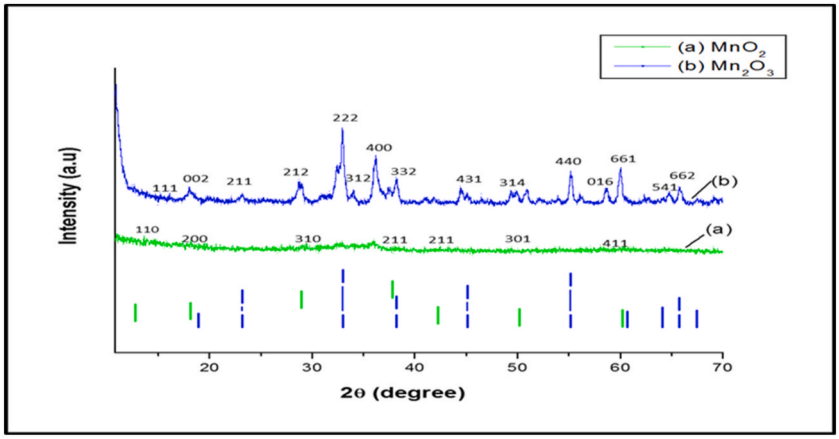

Fig. 3. XRD spectra of Mn_xO_y nanoparticles calcine at high temperatures of 600 °C (a) MnO_2 and 800 °C (b) Mn_2O_3.

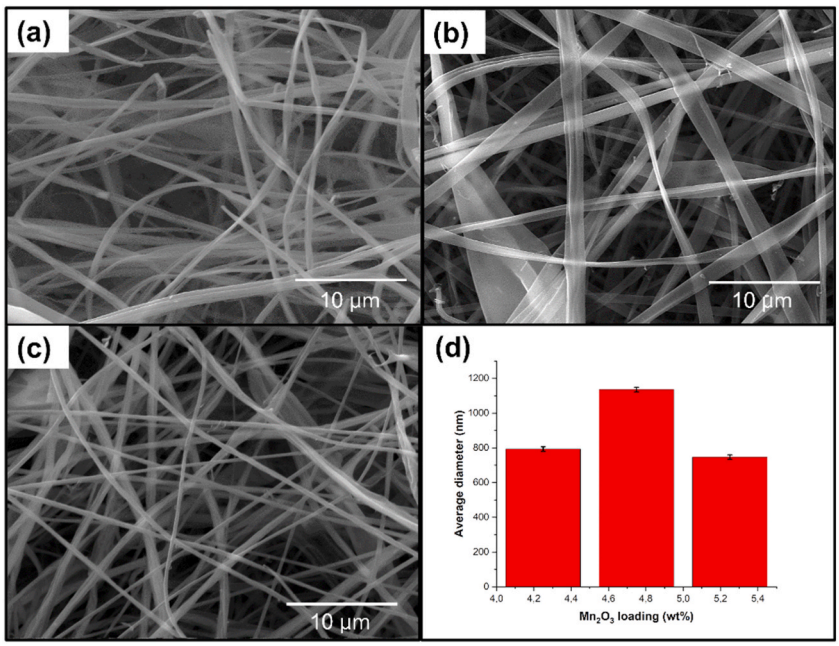

Fig. 4. SEM images and fiber size distribution of Mn_2O_3/zein/PVA nanocomposites with different loading of the nanoparticles (a) 4.25 wt% (b) 4.75 wt% (c) 5.25 wt%. Voltage: 25 kV and working distance: 10 cm.

nanocomposite blend increased significantly due to poorly dispersed Mn_2O_3 nanoparticles influenced by the amphiphilic nature of the zein/PVA fiber blends which corresponds to a similar study conducted in the article [19]. A decline in the averaged fiber diameter to 747 ± 1.29 nm was observed at the highest amount of the loadings (5.25 wt%) (Fig. 4(c)) resulting from improved dispersion, increased surface area, conductivity, and stronger interaction between the nanoparticles and the composite fiber blends although the exact mechanism of growth and corresponding kinetics of the formation of such structures is not clear [15,20,21]. Article [22] studied four types of metallic nanoparticles (gold, silver, silver-shelled-gold, and a mixture of gold and silver nanoparticles) embedded into zein/acrylamide nanofibers. An increase in concentration of the nanoparticles was observed to have sufficient influence in the distribution uniformity of the nanofibers therefore this observation correlated to the morphological observations of the current study. Furthermore, observations of the current study illustrates that conductivity and fiber diameter have an inverse relationship, higher conductivity of Mn_2O_3/zein/PVA solutions produced thinner diameter fibers due to increased electrostatic force and jet elongation [23].

3.2.2. Optical properties of Mn_2O_3 nanoparticles on zein/PVA fiber blends

Metal oxide nanoparticles embedded onto polymer fiber blends show distinctive properties, different from the individual metal

oxide nanoparticles. Article [18] studied the impact of morphology and optics of MnS/polyvinylcarbazole composites and it was reported that there was a strong interaction between the nanoparticles and the polymer while the absorption and photoluminescence spectra showed improvements. Fig. 5(a) and (c) displayed an excitonic peak at 320 nm that is blue shifted for 4.25 wt% Mn_2O_3/-zein/PVA with a band edge of 332 nm (3.73 eV), this may be due to the quantum effect. The bulk of 4.75 wt% Mn_2O_3/zein/PVA with a band edge of 413 nm (3.64 eV) displayed an excitonic peak at 322 nm which was red shifted from the 4.25 wt% Mn_2O_3/zein/PVA, this may be due to the quantization of energy levels causing an increase in the band gap energy. Mn_2O_3/zein/PVA nanocomposite fiber blends prepared at 5,25 wt% displayed an excitonic peak at 319 nm that was blue-shifted and broader with a band edge of 311 nm and a sufficiently increased band gap of 3.98 eV. The high absorbance illustrates that there was a decrease in the nanoparticle size at higher pH of Mn_2O_3 nanoparticles [29–30]. Fig. 5(b) is the photoluminescent results which displayed peaks at 431, 459, and 493 nm for the different concentrations of Mn_2O_3/zein/PVA nanocomposite fiber blends. Lower percentages of the blends gave a blue shift in contrast to red shifts observed for the higher concentrations. The 5.25% gave rise to smoother morphology and decreased fiber diameter compared to other concentrations of Mn_2O_3/zein/PVA nanocomposite fiber blends, an observation supported by the SEM images (Fig. 5). According to the article [20] studies on the physiochemical and optical properties of polyindole-bixybyte nanocomposite (Mn_2O_3/PI) with a direct band gap were reported to decrease with hybrid formation from 4.4 eV PI to 3.3eV Mn_2O_3/PI. Therefore, the deviation of other research studies previously conducted in this study factors such as the morphological structure, quantum confinement of the nanoparticles, and band gap energies of the nanocomposite materials.

3.2.3. *FTIR spectra of Mn_2O_3 nanoparticles on zein/PVA fiber blends*

The FTIR spectra (Fig. 6(a)-(c)) of Mn_2O_3/zein/PVA showed the characteristic absorption band of hydrogen bond recorded as 3291, 3289, and 3288 cm^{-1} for 4.25 wt%, 4.75 wt%, and 5.25 wt%. The C═O stretching frequency observed at 1644 cm^{-1} confirmed strong intermolecular interaction among amide groups in α-Mn_2O_3/zein/PVA. The amide II of zein fibers appeared at 1532, 1536 and 1516 cm^{-1} which indicates that loading manganese oxide does not disrupt the -α -helical structure of zein. In the article [24] studies on the synthesis and characterization of Mn/polyaniline nanocomposites via in situ approach were conducted and it was reported that the FTIR spectra of the PANI/MnO_2 nanocomposite had a band in the regions over 700 cm^{-1} which were assigned to Mn–O stretching

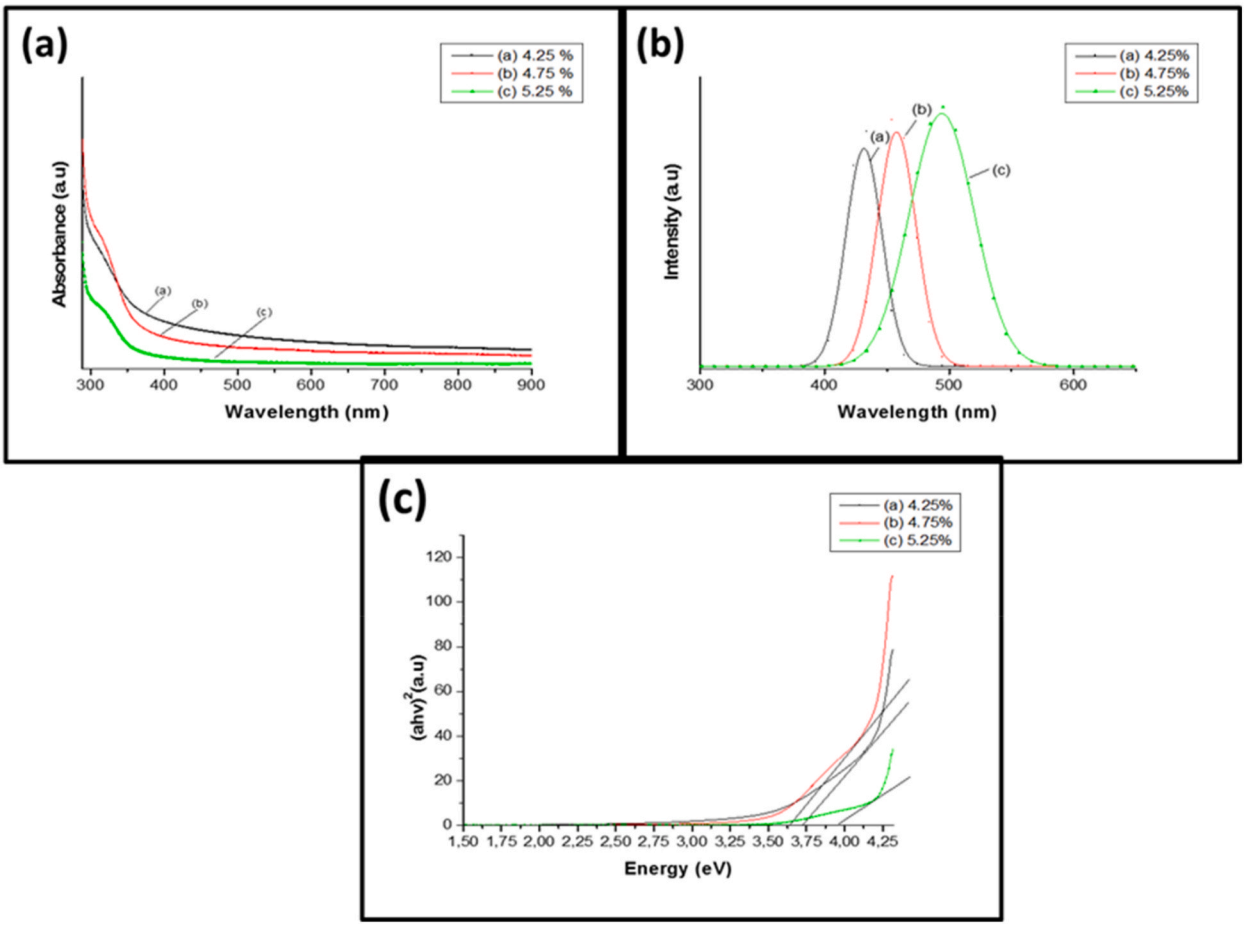

Fig. 5. (a) UV spectra (a) of Mn_2O_3/zein/PVA nanocomposites, (b) Photoluminescence spectra of Mn_2O_3, and (c) Tauc plot for direct transitions.

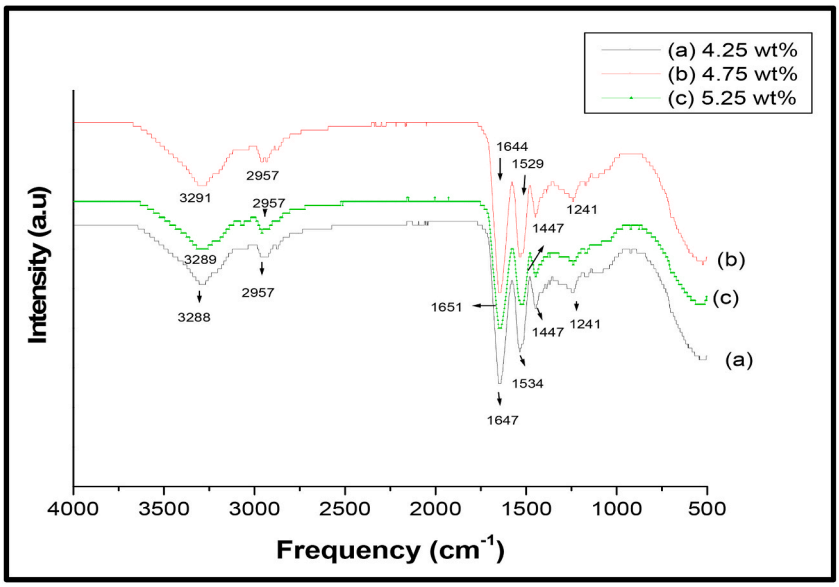

Fig. 6. FTIR spectra of α-Mn_2O_3/zein/PVA fiber blends with different concentrations of α-Mn_2O_3 nanoparticles (a) 4.25 wt %, (b) 4.75 wt %, and (c) 5.25 wt%.

vibrations. The lower percentage of the loadings of nanoparticles in this study do not appear to have great influence in the interaction or changes in the functional groups of the polymers. Therefore, manganese oxide was not observed around the fingerprint region. Article [22]. reported on the functional group peaks obtained from Raman spectroscopy. It was confirmed that major acrylamide peaks were seen at 1456 cm^{-1} (CH bending), 1315 cm^{-1} (CN stretching), 1165 cm^{-1} (NH_2 rocking), and 857 cm^{-1} NH_2 wagging) and the peak at 1456 cm^{-1}, confirmed the presence of acrylamide. Some acrylamide peaks are overlapping with some of the zein peaks. The peaks obtained for zein nanofibers for this study were in accordance with other reported studies [18,22,23].

3.2.4. Thermogravimetric analysis (TGA) of Mn_2O_3 nanoparticles on zein/PVA fiber blends

The thermal analysis (TGA, DTA) of the α-Mn_2O_3/zein/PVA nanocomposite was carried out from 30 to 900 °C. Fig. 7(a) depicts three weight loss for 4.25 wt% α-Mn_2O_3/zein/PVA nanocomposite, the first stage is about 4.15% below 100 °C which is due to evaporation of moisture in the material. A sharp weight loss of 59.18% occurred between 271 and 416 °C, which was due to the decomposition of zein/PVA. Another weight loss was observed between 416 and 592 °C, which was due to the decomposition of α-Mn_2O_3 nanoparticles present in the nanofiber blends. Fig. 7(b) depicts three weight loss of about 4.54% below 100 °C for 4.75 wt% α-Mn_2O_3/zein/PVA nanocomposite and a sharp major weight loss of 62.76% was observed between 244 and 308 °C. The third thermal decomposition occurred between 464 °C and 563 °C this may be due to the decomposition of zein/PVA fiber blend, and the final decomposition observed at 563–700 °C may be due to the complete decomposition of α-Mn_2O_3 nanoparticles. Fig. 7(c) depicts a weight loss of about 4.96% below 100 °*C* for 4.75 wt% α-Mn_2O_3/zein/PVA nanocomposite and a sharp major weight loss of 49.22% was observed between 279 and 346 °C. The third thermal decomposition occurred between 421 and 558 °C which could be due to the decomposition of zein/PVA fiber blend. The final decomposition observed at 563–776 °C may be attributed to the complete decomposition of α-Mn_2O_3 nanoparticles. 5.25 wt% was observed to be thermally stable due to enhanced cross-linking bonds and the prolonged final decomposition stages this may be attributed to the increment content of α-Mn_2O_3 nanoparticles into zein/PVA fiber blends. As a result, the effect of concentration has an influence on the rate of degradation demonstrating the influence of zein content in thermal properties. According to literature compactness of homopolymers in the nanofiber matrix influences the thermal and mechanical characteristics of the nanofibers [15,25,26]. The results obtained are similar to article [19,27].

4. Conclusion

Manganese oxide (Mn_2O_3 and MnO_2) was successfully synthesized using the co-precipitation method by varying temperatures. Their optical properties showed nanosized features from their band edges whereas TEM revealed the spherical and rod-shaped particles at 600 and 800 °C, respectively. This emphasized that temperature enhanced the shape and dimensions, and phase of the nanoparticles which was also confirmed by XRD. The effect of concentration of the incorporated Mn_2O_3 nanoparticles into zein/PVA fiber blends was studied using SEM, TGA, and XRD. It was demonstrated that the morphology of the fiber blends improved with increasing content of nanoparticle loadings and the electrospinnability of the nanocomposite fibers was enhanced. The nanoparticle concentrations were below the XRD detection limit since no patterns were observed from the samples except the background of the sample holder and amorphous nature of the polymers. The FTIR spectra showed no significant change in the functional group changes of the fiber blends upon loading with the lower concentrations of manganese nanoparticles. TGA demonstrated that nanoparticle

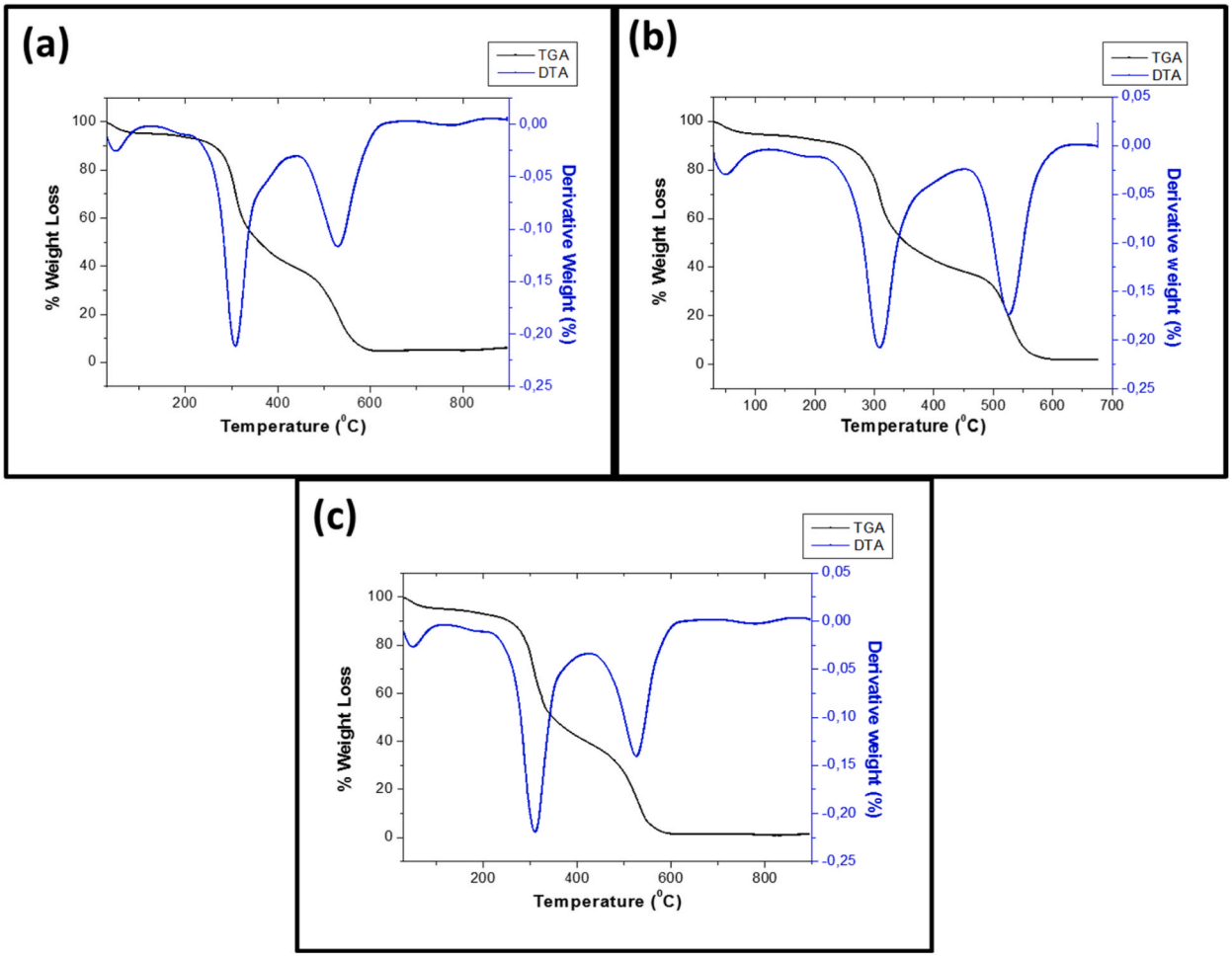

Fig. 7. TGA-DTA thermograms of α-Mn_2O_3/zein/PVA fiber blends with different concentrations of α-Mn_2O_3 nanoparticles (a) 4.25 wt %. (b) 4.75 wt % and (c) 5.25 wt% electrospun at 25 kV and distance: 10 cm.

loading enhanced the thermal stability of the electrospun α-Mn_2O_3/zein/PVA nanocomposite. SEM and UV Visible spectra revealed changes that demonstrate the presence of manganese oxide loaded on the fibres. Therefore, this study it was demonstrated that the embedment of manganese oxide nanoparticles into zein/PVA fiber blends enhanced the electrospinnability and morphology of the fiber blends.

Author contribution statement

Nompumelelo Mbali Kubheka: Conceived and designed the experiments; Performed the experiments; Analyzed and interpreted the data; Wrote the paper. Makwena Justice Moloto: Conceived and designed the experiments; Analyzed and interpreted the data; Contributed reagents, materials, analysis tools or data.

Data availability statement

Data included in article/supplementary material/referenced in article.

Declaration of competing interest

The authors declare that they have no known competing financial interests or personal relationships that could have appeared to influence the work reported in this paper.

Acknowledgements

The authors express their gratitude to the Vaal University of Technology for providing laboratory space, equipment and financial support. We would like to also thank NRF for funding the project and the nanotechnology group.

References

[1] S.G. Sanfélix, Manganese Oxide Nanoparticles : Synthesis and Magnetic Properties Erasmus Exchange, Technical Report, vols. 07–08, Philipps Universitat Marburg, 2016.
[2] Z.Y. Yuan, T.Z. Ren, G. Du, B.L. Su, A facile preparation of single-crystalline α-Mn_2O_3 nanorods by ammonia-hydrothermal treatment of MnO_2, Chem. Phys. Lett. 389 (2004) 83–86, https://doi.org/10.1016/j.cplett.2004.03.064.
[3] X. Shen, Z. Ji, H. Miao, J. Yang, K. Chen, Hydrothermal synthesis of $MnCO_3$ nanorods and their thermal transformation into Mn $_2O_3$ and Mn_3O_4 nanorods with single crystalline structure, J. Alloys Compd. 509 (2011) 5672–5676, https://doi.org/10.1016/j.jallcom.2011.02.119.
[4] M. Goodarz, H. Bahrami, M. Sadighi, S. Saber-Samandari, Quasi-static indentation response of aramid fiber/epoxy composites containing nylon 66 electrospun nano-interlayers, J. Ind. Text. 47 (2018) 960–977, https://doi.org/10.1177/1528083716679158.
[5] D.S. More, M.J. Moloto, N. Moloto, K.P. Matabola, TOPO-capped silver selenide nanoparticles and their incorporation into polymer nanofibers using electrospinning technique, Mater. Res. Bull. 65 (2015) 14–22, https://doi.org/10.1016/j.materresbull.2015.01.030.
[6] S. Torres-giner, E. Gimenez, J.M. Lagaron, Characterization of the morphology and thermal properties of Zein Prolamine nanostructures obtained by electrospinning, Food Hydrocol. 22 (2008) 601–614, https://doi.org/10.1016/j.foodhyd.2007.02.005.
[7] M. Zhang, Y. Liu, H. Yi, J. Luan, Y. Zhang, H. Cai, D. Sun, The Journal of the Textile Institute Electrospun zein/PVA fibrous mats as three- dimensional surface for embryonic stem cell culture, J. Text. Inst. 105 (2014) 246–255, https://doi.org/10.1080/00405000.2013.835902.
[8] M.L. Senna, S. Salmieri, S.A. Abdel-wahab El-naggar, M. Lacroix, A.G.S. Afrany, Acroix, Improving the compatibility of zein/poly (vinyl alcohol) blends by gamma irradiation and graft copolymerization of acrylic acid, J. Agric. Food Chem. 58 (2010) 4470–4476, https://doi.org/10.1021/jf904088y.
[9] B. Jie, L. Chunping, W. Shan, A novel approach to prepare gold nanoparticles/polyacrylamide composite nanofibers, Rare Met. Mater. Eng. 42 (2013) 474–477, https://doi.org/10.1016/S1875-5372(13)60051-X.
[10] S.C. Nkabinde, M.J. Moloto, K.P. Matabola, Optimized loading of TiO $_2$ nanoparticles into electrospun polyacrylonitrile and cellulose acetate polymer fibers, J. Nanomater. 2020 (2020), https://doi.org/10.1155/2020/9429421.
[11] S. Zargham, S. Bazgir, A. Tavakoli, A.S. Rashidi, R. Damerchely, The effect of flow rate on morphology and deposition area of electrospun nylon 6 nanofiber, J. Eng. Fiber. Fabr. 7 (2012) 42–49, https://doi.org/10.1177/155892501200700414.
[12] P.W. Yu, Development of Nanostructured Materials Based on Manganese Oxides and Produced by an Electrochemical Method for Water Electrolysis, Univ. Pierre Marie Curie Chim., 2016.
[13] D. Portehault, S. Cassaignon, J. Jolivet, Structural and morphological control of manganese oxide nanoparticles upon soft aqueous precipitation through MnO_4 À/Mn^{2+} reaction, J. Mater. Chem. 19 (2009) 2407–2416, https://doi.org/10.1039/b816348k.
[14] A.M. Fayaz, K. Balaji, M. Girilal, R. Yadav, P.T. Kalaichelvan, R. Venketesan, Biogenic synthesis of silver nanoparticles and their synergistic effect with antibiotics : a study against gram-positive and gram-negative bacteria, Nanomed. Nanotechnol. Biol. Med. 6 (2010) 103–109, https://doi.org/10.1016/j.nano.2009.04.006.
[15] M. Aman Mohammadi, S. Ramezani, H. Hosseini, A.M. Mortazavian, S.M. Hosseini, M. Ghorbani, Electrospun antibacterial and antioxidant zein/polylactic acid/hydroxypropyl methylcellulose nanofibers as an active food packaging system, Food Bioprocess Technol. 14 (2021) 1529–1541, https://doi.org/10.1007/s11947-021-02654-7.
[16] E. Lee, T. Lee, B.S. Kim, Electrospun nanofiber of hybrid manganese oxides for supercapacitor: relevance to mixed inorganic interfaces, J. Power Sources 255 (2014) 335–340, https://doi.org/10.1016/j.jpowsour.2014.01.011.
[17] N.H. Von Reitzenstein, X. Bi, Y. Yang, K. Hristovski, P. Westerhoff, Morphology , structure , and properties of metal oxide/polymer nanocomposite electrospun mats, Appl. Polym. Sci. 133 (2016) 1–9, https://doi.org/10.1002/app.43811.
[18] C. Joaqu, A review of zein as a potential biopolymer for tissue engineering and nanotechnological applications, Processes 8 (2020) 121, https://doi.org/10.3390/pr8111376.
[19] R. Najjar, R.A.A.M. Abdel-gaber, Physical properties of Mn_2O_3 nanoparticles synthesized by Co-precipitation method at different pH values, J. Supercond. Nov. Magnetism 32 (2018) 885–892, https://doi.org/10.1007/s10948-018-4765-x.
[20] B.B.P. Rejania, Structural and nanocomposite optical properties of polyindole-manganese oxide nanocomposite, Indian J. Adv. Chem. Sci. 2 (2013) 244–248.
[21] U. Chatterjee, S.K. Jewrajka, S. Guha, Dispersion of functionalized silver nanoparticles in polymer matrices : stability , characterization , and physical properties, Polym. Compos. 30 (2009) 827–834, https://doi.org/10.1002/pc.20655.
[22] H. Turasan, M. Cakmak, J. Kokini, A disposable ultrasensitive surface enhanced Raman spectroscopy biosensor platform fabricated from biodegradable zein nanofibers, J. Appl. Polym. Sci. 139 (2022) 1–13, https://doi.org/10.1002/app.52622.
[23] Z. Cetinkaya, Turgay wijaya, wahyu altay, filiz ceylan, fabrication and characterization of zein nanofibers integrated with gold nanospheres, Food Sci. Technol. 155 (2022), https://doi.org/10.1016/j.lwt.2021.112976.
[24] V.B. S.C.Vella Durai Prasad, L. Guru, E. Kumar, D. Muthuraj, Jothy, synthesis and characterization of Mn/polyaniline nanocomposites via in situ approach, Int. J. Adv. Res. Sci. Eng. 7 (2018) 781–790.
[25] K. Swaroop, H.M. Somashekarappa, Effect of pH values on surface Morphology and Particle size variation in ZnO Nanoparticles Synthesised by co-precipitation Method Effect of pH values on surface Morphology and Particle size variation in ZnO Nanoparticles Synthesised by co-precipitation Me, Res. J. Recent Sci. 4 (2015) 197–201.
[26] S. Goodarz, M. Bahrami, S.H. Sadighi, M. Saber-Samandari, The influence of graphene reinforced electrospun nano-interlayers on quasi-static indentation behavior of fiber-reinforced epoxy composites, Fibers Polym. 18 (2017) 322–333, https://doi.org/10.1007/s12221-017-6700-3.
[27] N. Moloto, N.J. Coville, S. Sinha, M.J. Moloto, Morphological and optical properties of MnS/polyvinylcarbazole hybrid composites, Phys. B Phys. Condens. Matter. 404 (2009) 4461–4465, https://doi.org/10.1016/j.physb.2009.09.040.